© 1991 Oxford University Press

Nucleic Acids Research, Vol. 19, No. 23 6519–6525

Self-cleavage of a 71 nucleotide-long ribozyme derived from hepatitis delta virus genomic RNA

Gilbert Thill[1], Marta Blumenfeld[1], Franck Lescure[1,2] and Marc Vasseur[1,2,*]
[1]GENSET, 1 passage Etienne Delaunay, 75011 Paris and [2]Laboratoire de Virologie Moléculaire, Université Paris VII, 2 place Jussieu, 75251 Paris Cédex 05, France

Received August 12, 1991; Revised and Accepted November 8, 1991

ABSTRACT

Self-cleavage efficiency of ribozymes derived from hepatitis delta virus (HDV) has been shown to depend on the RNA structure, which in turn may be determined by the length of the considered sequences. Here we describe the construction and functional analysis of a 71 nucleotide-long RNA genomic fragment, Rz71, which carries an 18 nucleotide deletion in a very stable GC-rich stem-loop (stem IV), predicted to be present in several computer-derived secondary structure models. Rz71 is able to undergo self-cleavage under non-denaturing conditions (the $t_{1/2}$ of the reaction at 37°C is 3 min). The deletion, however, is not neutral, since under the same conditions the non-deleted ribozyme cleaves to 50% in less than 15 sec. Therefore, stem-loop IV seems to play a structural role, not being directly involved in the catalytic reaction, but contributing to the correct positioning of the catalytic core of the HDV ribozyme. Rz71 is the smallest self-cleaving sub-fragment of HDV genomic RNA reported so far.

INTRODUCTION

Hepatitis Delta Virus (HDV) is a human pathogen present in some severe hepatitis B patients (1). HDV contains a circular, single-stranded RNA genome of 1.7 kilobases (2–4), which has the ability to fold into an unbranched, rod-like structure under non-denaturing conditions (2,3). Many of these HDV features are similar to those of some pathogenic RNAs of plants, and this similarity also includes the ability of both genomic and antigenomic HDV RNA strands to undergo site-specific self-cleavage and ligation (reviewed in 5). The autocleavage and ligation of antigenomic and genomic RNAs, both *in vivo* and *in vitro* (6–10), supports the idea that HDV RNA replicates through a rolling circle mechanism (10).

HDV self-cleavage reactions can be performed by short viral RNA fragments of 100–150 bases (7,8). The reaction is a site-specific transesterification, producing a 3′ fragment with 5′OH and a 5′ fragment with 2′,3′-cyclic monophosphate (7,8). As in plant pathogens, RNA self-cleavage requires the presence of a divalent cation, such as Mg^{++}; maximum cleavage is observed at very low Mg^{++} concentrations (0.05–0.1 mM; ref.11). More strikingly, the reaction rate can be enhanced by increasing the reaction temperature up to 80°C (11–13) or by adding denaturant agents (up to 15 M or 18 M formamide and up to 8 M or 10 M urea, for genomic or antigenomic HDV, respectively; 11,13). Moreover, HDV ribozyme activity is highly influenced by the presence of both HDV internal and non-HDV flanking sequences (7,8,14).

The smallest RNA subfragment from the genomic HDV strand that can self-cleave was postulated to contain only 1 nucleotide (nt) 5′ to the break site and either 82 nt or, in the presence of denaturants, 84 nt 3′ to the break site (15). Perrotta and Been have shown that an *in vitro* transcribed RNA containing 88 nt (−3 to +85) from the genomic HDV strand plus 18 bases of 3′ vector derived sequences was able to self-cleave at 37°C . Since the self-cleavage rate could still be enhanced by the addition of denaturants (the $t_{1/2}$ of the reaction was about 3.5 min in the absence of denaturants and 0.2 min in 40% formamide; ref. 15), it was postulated that at least part of this enhancement resulted from destabilizing inhibitory structures generated by sequences flanking the self-cleavage site.

Sequence and structural analysis of HDV self-cleaving domains show no homologies with previously described ribozyme motifs, such as hammerhead or hairpin-like structures (16,17), thus suggesting that the HDV ribozymes represent a new type of autocleaving RNA. Perrotta and Been have recently proposed a secondary structure model for both the genomic and antigenomic HDV minimal self-cleaving fragments, which takes into account a tertiary interaction between an internal loop and 3′ terminal sequences to generate a pseudoknot-like structure (Fig.1-A, Rz85/pseudoknot; 18). By performing deletion and site-specific mutagenesis analysis on the antigenomic ribozyme, they concluded that the pseudoknot interaction (stem II in Figure 1-A) is not essential for cleavage under favourable conditions (in the absence of denaturants), but can stabilize the self-cleaving structure (18).

We were interested in further analyzing the structure-function relationship of the HDV genomic ribozyme by performing

* To whom correspondence should be addressed at Laboratoire de Virologie Moléculaire, Université Paris VII, 2 place Jussieu, 75251 Paris Cédex 05, France

internal deletions on the minimal Rz85 self-cleaving fragment. Here we present evidence that self-cleavage still occurs even after partial deletion of stem IV (see Fig.1-A), thus assigning a non catalytic, but structural role for this particular hairpin.

MATERIALS AND METHODS

Production of T7/HDV DNA templates by PCR

HDV genomic RNAs used in this study (Figure 2A) were obtained as follows. DNA oligonucleotides Rz89 (−5 to +84 with respect to the genomic cleavage site, corresponding to positions 681 to 769 from genomic HDV; ref. 2) and Rz71 (Rz89 deleted from nt +51 to +68) were synthesized on an Applied Biosystems synthesizer, deprotected with ammonia, precipitated with ethanol and used without further purification in a polymerase chain reaction (PCR, Perkin-Elmer Cetus protocol) to amplify the corresponding double stranded HDV sequences. The 5′ PCR primer (5′CGCCGGATCCTAATACGACTCACTATAGCTG-ATGGCCGGCATGGT3′) contained a BamHI site and the T7 promoter (20), followed by 17 nucleotides (−5 to +12) of HDV sequences; the 3′ primer was complementary to the 3′ 17 bases of the HDV oligonucleotides. Amplification reactions contained 10 mM Tris HCl pH 8.4, 50 mM KCl, 1.5 mM $MgCl_2$, 0.01% gelatin, 200 μM each dNTP, 100 pg/ml to 1μg/ml of crude single stranded template, 0.6 μM of each primer and 25 U/ml Taq DNA polymerase. Reaction mixtures were denatured for 5 min at 94°C; amplification conditions were: 94°C 1 min, 50°C 1 min, 72°C 1 min, 5 cycles; 90°C 1 min, 50°C 1 min, 72°C 1 min, 30 cycles. Amplification products were separated by gel electrophoresis on 10% acrylamide native gels, bands were visualized by UV shadowing, and products of the expected size were eluted, extracted with phenol and recovered by ethanol precipitation, following standard procedures (19).

Synthesis of HDV self-cleaving precursor RNAs

HDV RNAs were synthesized by T7 RNA polymerase transcription of PCR-produced DNA templates. For transcription of nonradioactive RNA, a 50 μl reaction contained 40 mM Tris HCl (pH 8.0), 8 mM $MgCl_2$, 2 mM spermidine, 50 mM NaCl, 30 mM DTT, 1.2 mM each of ATP, CTP, GTP and UTP, 40 units of RNAGuard (Pharmacia), 70−120 pmol/ml of template DNA and 50 units of T7 RNA polymerase (Boehringer Mannheim). Where indicated, GTP was replaced by 12 mM ITP. For radiolabeled transcription, the UTP concentration was lowered to 40 μM, and 50 μCi (α-^{32}P) UTP (800 Ci/mmol, Amersham) were included. Reactions were incubated for 1 hour at 37°C or 24−48 hours at 4°C, as indicated. After incubation, reactions were terminated by adding an equal volume of 50 mM EDTA/95% formamide, and transcription products were fractionated by electrophoresis on an 8% acrylamide/7M urea gel. RNA bands corresponding to full-length precursors or 3′ cleavage products (see text) were located by UV shadowing or autoradiography, eluted overnight at room temperature in 0.75 M ammonium acetate, 1 mM EDTA, 0.1% SDS and recovered by ethanol precipitation. RNA was resuspended in 1 mM EDTA and stored at −20°C.

5′ end-labeling of transcripts

Gel-purified RNA fragments were treated with calf intestinal phosphatase in 50 mM TrisHCl pH 8.0, 1 mM EDTA for 30

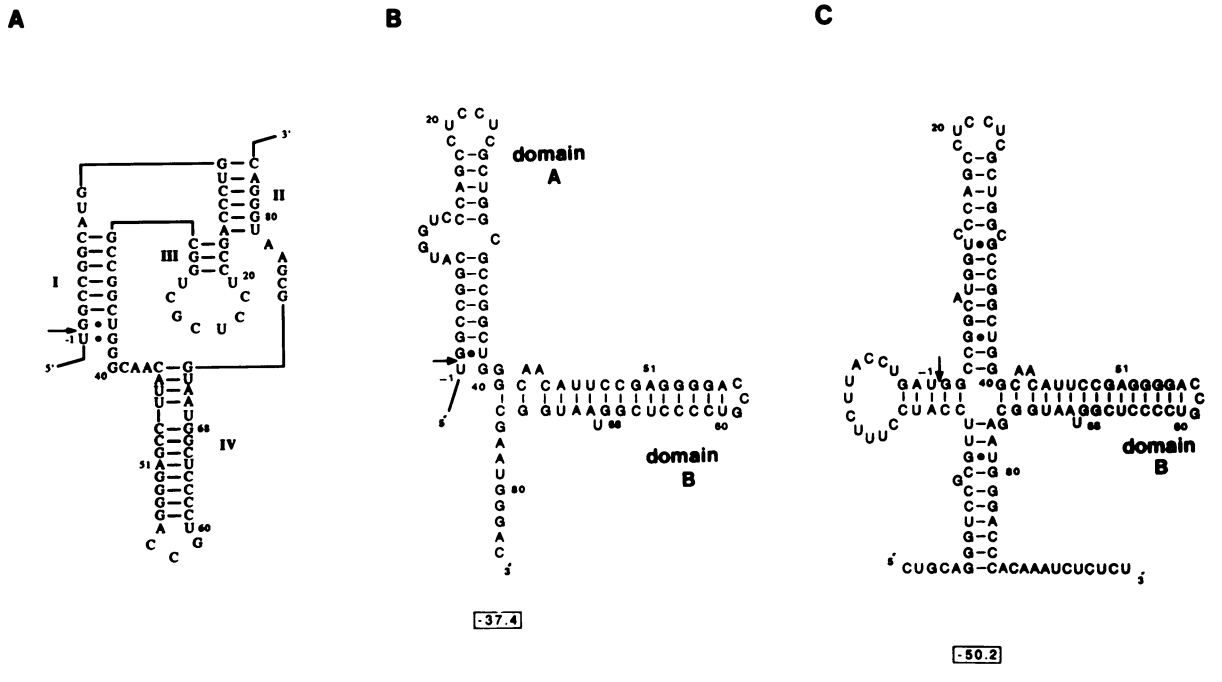

Figure 1. Potential secondary structures for HDV genomic self-cleaving RNAs. The sequences are numbered from the cleavage-site (marked by an arrow). Watson−Crick base-pairs are indicated by dashes, wobbles by dots. In **A** is represented the pseudoknot-like structure proposed by Perrotta and Been (18) for an 85 nt-long HDV genomic ribozyme (−1 to +84); **I** to **IV** indicates the stem-loop regions (see text). **B** and **C** show the potential secondary structures obtained by the RNAFOLD program (24). In **B** is depicted the lowest free energy structure of Rz85 (G_0= −37.4 kcal); **C** shows the most stable secondary structure calculated for Rz133 (−35 to +98; G_0= −50.2 kcal). Domain A and B correspond to nucleotides −1 to +40 and +44 to +73, respectively (see text). Positions 51 to 68 indicate the region deleted in Rz71 (see text).

min at 37°C, and then phosphorylated with T4 polynucleotide kinase and (γ-^{32}P) ATP (3000 Ci/mmol, Amersham) in 50 mM TrisHCl pH 7.5, 10 mM $MgCl_2$, 1 mM spermidine, 5 mM DTT for 3 h at 4°C. The reaction was stopped by adding an equal volume of 50 mM EDTA, 95% formamide and the 5′ end-labeled RNA was purified by gel electrophoresis as described above. RNA concentrations were estimated by liquid scintillation counting.

Self-cleavage reactions

5′ (^{32}P) RNA was denatured at 95°C for 1 min in 1 mM EDTA, followed by quick cooling on ice. Reactions were initiated by addition of 40 mM TrisHCl pH 8.0, 10 mM $MgCl_2$ and carried out at the indicated temperatures. Aliquots of 5 μl were removed at various time intervals and reactions were stopped by addition of an equal volume of 50 mM EDTA/95% formamide. Samples were heated at 95°C for 1 min and loaded on a 10% acrylamide/7 M urea gel. After electrophoresis, the gel was transferred to filter paper, dried, and exposed to X-ray film. The bands corresponding to full-length precursors and 5′-cleaved products were located by use of the autoradiograph, excised and quantified by Cerenkov counting. Percentage of cleavage was determined by taking as 100% the radioactivity of the full-length precursor plus the 5′-cleaved product for each time point.

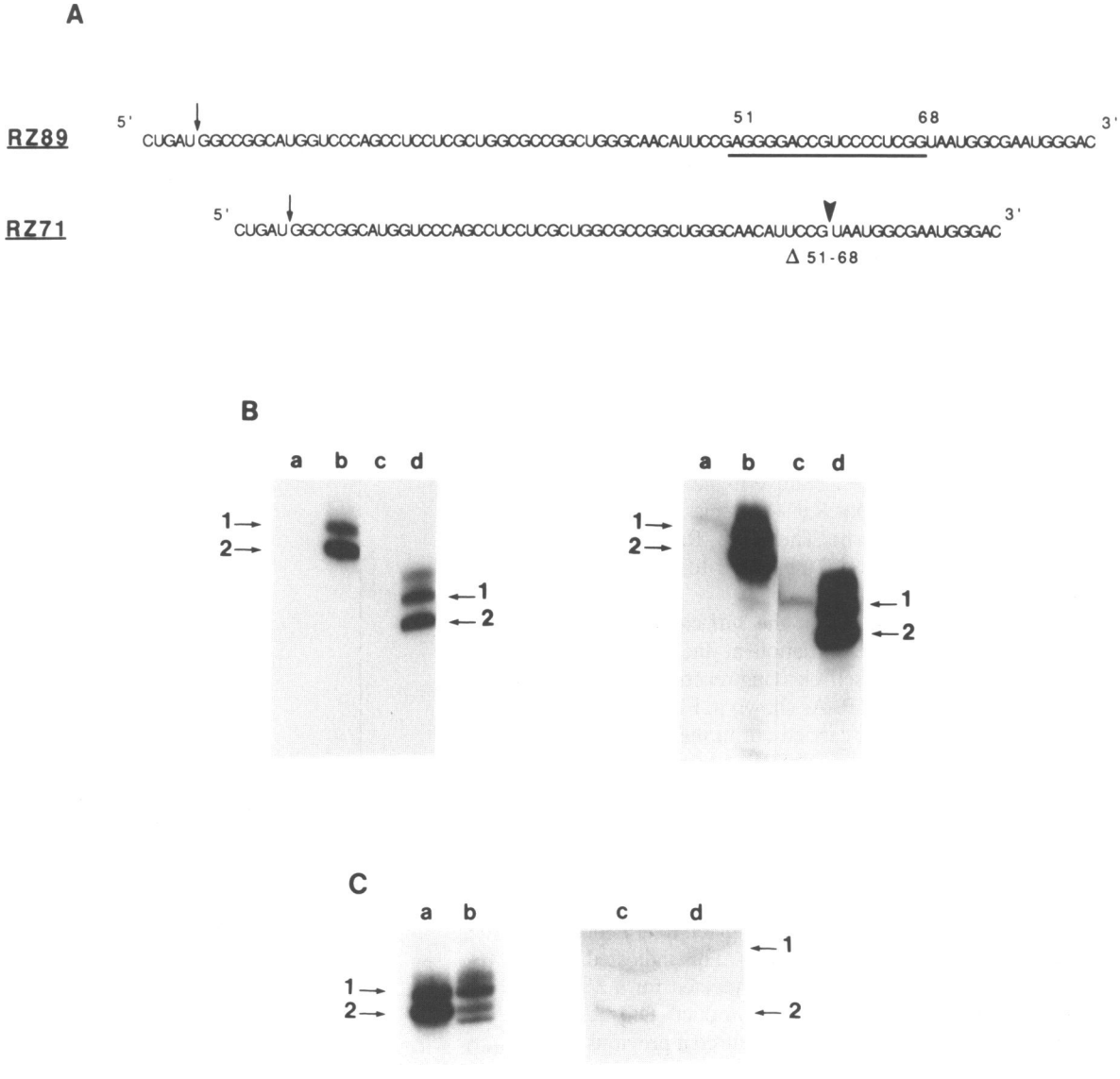

Figure 2. Analysis of products obtained after transcription of PCR-produced DNA templates. DNA template preparation and transcription conditions were as described in Mat. & Meth. Panel **A** shows the sequence of the HDV genomic RNAs Rz89 and Rz71; arrows indicate the cleavage site; sequences from Rz89 deleted in Rz71 are underlined (51 to 68) and the position of the deletion is indicated by an arrowhead (Δ51−68). In panel **B**, Rz89 (lanes a and b) and Rz71 (lanes c and d) PCR-produced templates were transcribed for 1 h at 37°C in the presence of (α-^{32}P) UTP and either 1.2 mM GTP (lanes b and d) or 12 mM ITP (lanes a and c), and products were analyzed by PAGE 10%/7M urea as described in Mat. & Meth.. The left photograph shows a short autoradiographic exposure, the right photograph, a longer one. In panel **C**, Rz89 DNA template was transcribed for 1 h at 37°C (lanes a and c) or 48 h at 4°C (lanes b and d), in the presence (lanes a and b) or absence (lanes c and d) of (α-^{32}P)UTP. After electrophoresis on a 8% acrylamide/7M urea gel, transcription products were visualized by autoradiography (lanes a and b) or UV-shadowing (lanes c and d). Arrows in **B** and **C** show the positions of the corresponding Rz89 and Rz71 full length transcripts (1) or 3′ cleavage products (2); see text.

RNA sequencing

In vitro transcribed RNAs were sequenced by the dideoxy sequencing method (19), using AMV reverse transcriptase (Boehringer Mannheim) and a 5′-(^{32}P)17-mer primer complementary to the 3′ end of the RNA molecules.

RESULTS

HDV89 self-cleaves efficiently during transcription

HDV DNA oligonucleotides (Fig.2-A) were synthesized and amplified by PCR to generate the corresponding double-stranded templates. The templates were designed so that, after transcription with T7 RNA polymerase, only one non-HDV nucleotide (a 5′ G corresponding to the transcription start site and required for efficient transcription; ref. 20), was incorporated in the final RNA transcripts.

By using this method, we first studied Rz89, a genomic HDV fragment containing 5 nt upstream of the cleavage site and 84 nt downstream (Fig.2-A). After transcription of the PCR-produced template, two RNAs were detected: a major band corresponding to 70−80% of the transcripts and a slightly slower migrating species (Rz89-2 and Rz89-1, respectively; Figure 2-B lane b). One explanation of this result was that Rz89 self-cleaved during transcription. Thus, the minor Rz89-1 RNA would be the 89 nt precursor whereas the most prominent Rz89-2 would correspond to the 3′ 84-base cleavage product. Alternatively, Rz89-2 could represent a prematurely terminated transcript.

In order to verify the identity of both transcripts, we analyzed the sequences of both Rz89-1 and Rz89-2 by primer extension with reverse transcriptase and dideoxy sequencing. Primer-extended products derived from the major Rz89-2 transcript predominantly stopped at position G+1 relative to the break site, while reverse transcription of the minor Rz89-1 species elongated to the 5′ end of Rz89 (data not shown). Therefore, Rz89-1 was the full-length ribozyme, while Rz89-2 appeared to be the 3′ cleavage product.

To confirm that Rz89-2 resulted from the self-cleavage of Rz89-1 and not from transcription initiation at the genomic cleavage-site, we tried to inhibit the self-cleaving reaction during transcription by replacing GTP by ITP. As shown in Figure 2-B, when radiolabeled transcription was carried out in the presence of ITP, a band comigrating with the Rz89-1 precursor was detected but no RNA was found at the position of Rz89-2, even after a long autoradiographic exposure (Fig.2-B right, compare lanes a and b).

In addition, when non-radioactive Rz89-2 was 5′ end-labeled with T4 polynucleotide kinase and (γ-^{32}P)ATP, the extent of phosphorylation was the same with or without prior treatment with calf intestinal phosphatase (data not shown). This indicated that Rz89-2 had a free 5′ hydroxyl group, as expected for a 3′ cleavage product and not for a transcription product. On the contrary, efficient 5′ end-labeling of Rz89-1 required a previous dephosphorylation step (results not shown). These results further supported the idea that Rz89-1 was the full-length Rz89 RNA, while Rz89-2 was its 3′ cleavage product.

The above data indicated that Rz89 was able to acquire the active conformation required for self-cleavage during the transcription reaction.

Transcription at 4°C provides a method for preparing uncleaved ribozyme precursors

When gel-purified Rz89-1 was incubated under various conditions known to cause efficient self-cleavage (1−10 mM Mg^{++}, 30−90°C), the RNA never cleaved to more than 10% (data not shown; see next section and Discussion). In order to obtain active full-length precursor to perform kinetic studies of the Rz89 cleavage reaction, we looked for transcription conditions that would prevent the self-cleavage of RNA transcripts.

As self-cleavage reactions depend on temperature, we thought that transcription at low temperature might affect more drastically the self-cleavage reaction than the transcription efficiency, then increasing the proportion of the uncleaved precursor. Figure 2-C shows that after unlabeled transcription at 4°C for 48 h, only the Rz89-1 precursor was detected, while no transcript was visualized at the position of the major Rz89-2 cleavage product obtained at 37°C (Fig.2-C, compare lanes c to d). When a radioactive transcription was similarly analyzed, the major transcription product was found at the position of the Rz89-1 precursor; two additional minor bands were also detected. The upper one, comigrating with Rz89-2, (Fig.2-C, lanes a and b), probably resulted from a residual cleavage still occuring at 4°C; the other one might result from an alternative cleavage site. Also, these bands could have resulted from pausing by RNA polymerase. We did not further investigate these hypotheses.

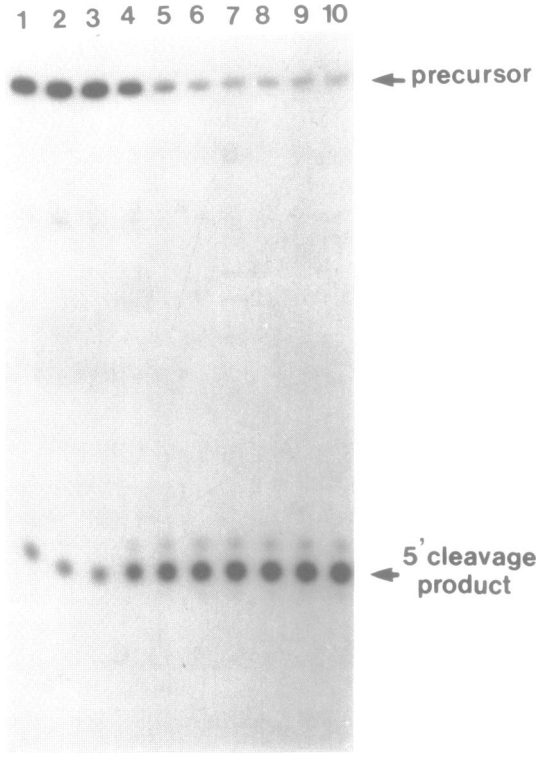

Figure 3. Self-cleavage of Rz89 at 37°C. The Rz89 precursor obtained by transcription at 4°C was 5′ end-labeled with (γ-^{32}P) ATP and was further gel-purified. The radioactive Rz89 was denatured at 95°C for 1 min in 1 mM EDTA (lanes 1,2, and 4 to 10) or 10 mM EDTA (lane 3) and snap-cooled on ice for 5 min. Tubes were then supplemented at 4°C with 40 mM Tris HCl pH 8.0 (lanes 2 and 3) or 40 mM Tris HCl pH 8.0 and 10 mM $MgCl_2$ (lanes 4 to 10), vortexed and spun down for 5 sec at room temperature, put again on ice and then incubated at 37°C. Aliquots were taken at time 0 (lane 4), 15 sec (lane 5), 30 sec (lane 6), 1 min (lane 7), 2 min (lane 8), 5 min (lane 9), 30 min (lanes 2 and 3) and 60 min (lane 10), and reactions were stopped by addition of 1 volume of 95% formamide/50 mM EDTA. In lane 1, the aliquot of (^{32}P)Rz89 was supplemented with formamide/EDTA gel loading buffer immediately after the snap-cool step. Samples were analyzed by PAGE 10%/7M urea as described in Mat. & Meth.

Kinetics of Rz89 self-cleavage reaction

To study the kinetics of Rz89 self-cleavage, we prepared full-length Rz89 as described above by carrying out at 4°C the Mg^{++}-dependent reactions (*i.e.*, transcription and kination), while the elution and dephosphorylation steps were performed in the presence of EDTA at room temperature and 37°C, respectively.

We then incubated 5′ end-labeled Rz89-1 with 10 mM $MgCl_2$ at 37°C, and followed the reaction time course by analyzing the cleavage products on a 10% polyacrylamide denaturing gel. As shown in Figure 3, 5′-(^{32}P)-Rz89-1 precursor cleaved very rapidly: 50% of the radioactivity was associated to the expected 5′ cleavage product in less than 15 sec and the reaction was completed after 1−2 min (Fig.3, lanes 5 to 10).

A cleavage-resistant precursor, corresponding to 1−5% of the original material, was systematically observed (Fig.3, lanes 6 to 10). It probably represents an inactive precursor generated by misincorporation and/or 3′ addition of non-template encoded nucleotides by T7 RNA polymerase, as already described for synthetic templates (20−23). The latter hypothesis might also explain the cleavage-resistance of Rz89-1 transcribed at 37°C. Also, the presence of a minor cleavage product, migrating slightly slower than the correct band (Fig.3, lanes 4 to 10), was not further investigated. It may represent the 5′ cleavage product of the putative alternative cleavage mentioned when describing Fig.2C, lane b (see above section).

Cleavage of Rz89 is so efficient that an aliquot taken immediately after the addition of $MgCl_2$ at 4°C, vortexed and subsequently supplemented with loading buffer, already contained 15−20% of cleaved product (Fig.3, lane 4). Moreover, 5−10% of the gel-purified 5′ end-labeled ribozyme seems to be cleaved during the overnight elution from the gel at room temperature in the presence of 1 mM EDTA (Fig.3, lane 1). However, the cleavage reaction at 37°C clearly depends on the presence of Mg^{++}, since controls incubated for 30 min at 37°C in the presence of 1 or 10 mM EDTA, showed no further cleavage than that observed in the original material (Fig.3, compare lanes 1 to 3). Finally, the extent of cleavage was not affected by decreasing the Mg^{++} concentration to 2 mM or when the ribozyme was not heat-denatured before the incubation (data not shown).

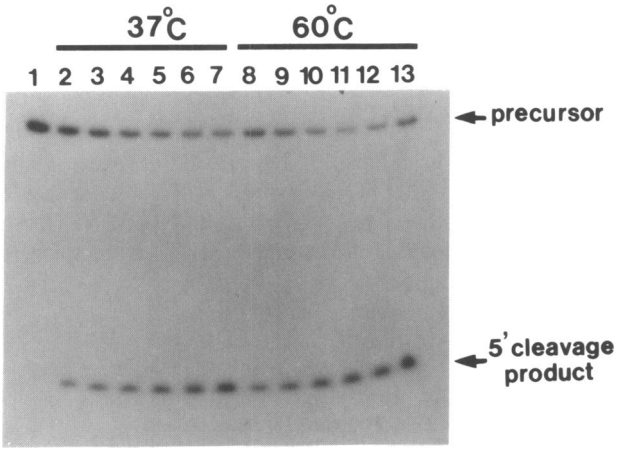

Figure 4. Self-cleavage of Rz71 at 37°C and 60°C. 5′ end-labeled Rz71, obtained as described for Rz89 (Fig.3), was denaturated at 95°C for 1 min in 1 mM EDTA, snap-cooled on ice, supplemented with 40 mM Tris HCl pH 8.0, 10 mM $MgCl_2$, and then incubated at 37°C (lanes 2 to 7) or 60°C (lanes 8 to 13). Aliquots were removed at 1 min (lanes 2 and 8), 2 min (lanes 3 and 9), 5 min (lanes 4 and 10), 10 min (lanes 5 and 11), 20 min (lanes 6 and 12) or 60 min (lanes 7 and 13); in the control (lane 1) the aliquot was removed before the addition of $MgCl_2$. The reactions were stopped with 1 volume of 95% formamide/50 mM EDTA, and samples were analyzed by PAGE 10%/7 M urea as described in Mat. & Meth.

Rz71 is the shortest HDV self-cleaving fragment described so far

By using the RNAFOLD program (24) to evaluate the potential secondary structures of the putative minimal ribozyme Rz85 (−1 to +84), we obtained several alternative conformations, with G_0 values ranging from −37.4 to −32.4 kcal (Fig.1-B and data not shown). A stable GC-rich stem-loop, extending from positions +44 to +73 (domain B, Fig.1-B), was systematically observed in all alternative structures (data not shown). This hairpin is also present in the pseudoknot-like structure proposed by Perrotta and Been (stem IV in Fig.1-A, Rz85/pseudoknot; 18). Moreover, the same stem region was also found in the Rz133 (−35 to +98) alternative conformations (G_0 varying from −50.2 to −38.2 kcal; Fig.1-C and results not shown). Rz133 is essentially inactive in the absence of denaturants or at moderate temperatures, and its self-cleaving capacity is highly influenced by 5′ and/or 3′ flanking sequences (11,12,14, and G.T. unpublished results).

To analyze the role of stem IV, and in order to test if this structure was part of the catalytic core of the HDV ribozyme, we studied the cleavage activity of an RNA molecule selectively deleted in this region.

We synthesized Rz71, a 71 nt-long Rz89-derived molecule, deleted in domain B from positions +51 to +68 (Fig.2-A). The procedure followed to obtain the deleted Rz71 RNA transcripts was similar to that previously described for Rz89. *In vitro* transcription of the PCR-amplified HDV71 template at 37°C gave rise to a faster migrating RNA and a slower transcript (Rz71-2 and Rz71-1, respectively; Fig. 2-B, lane d). A minor band, migrating above Rz71-1, was also present; it could result from 3′ additions by T7 RNA polymerase (20−23). Sequence analysis of both Rz-71-1 and Rz71-2 showed that Rz71-1 was the *bona fide* full length ribozyme, while Rz71-2 appeared to be the 66 nt 3′ cleavage product (data not shown). These data then suggested that Rz71 was able to self-cleave during transcription. This was further confirmed by performing transcription under the self-cleavage inhibition conditions described for Rz89, such as transcription in the presence of ITP or at 4°C (Fig.2-B, lanes c and d, and results not shown). In addition, Rz71-2 was easily phosphorylated with (γ-^{32}P)ATP even without previous phosphatase treatment, while efficient end-labeling of Rz71-1 required prior dephosphorylation (results not shown). Again, these observations indicated that Rz71-2 had a 5′OH and Rz71-1 a 5′-P, as expected for a 3′ cleavage product and a full-length precursor, respectively.

As for Rz89, to conclusively demonstrate that Rz71 was able to self-cleave, we prepared 5′ end-labeled Rz71 ribozyme obtained by transcription at 4°C, and incubated the purified (^{32}P)-RNA under cleavage-conditions. Figure 4 shows the time course corresponding to the incubation of Rz71 with 10 mM $MgCl_2$ at 37°C. Under this condition, Rz71 ribozyme self-cleaved with a $t_{1/2}$ of 3 min (Fig.4, compare lanes 2 to 7). The reaction could still be enhanced by partial denaturing conditions, since at 60°C and 10 mM $MgCl_2$ the observed $t_{1/2}$ was less than 2 min (Fig.4, lanes 8 to 13).

Therefore, Rz71 is the smallest HDV RNA subfragment able to self-cleave described so far.

DISCUSSION

An improved method for the synthesis of *in vitro* transcribed self-cleaving RNAs

A major limitation in the study of reactions that are highly dependent on molecular structure, such as RNA-involved processes, is that in most cases, the presence of potentially interfering vector sequences cannot be avoided. In the specific case of HDV ribozyme self-cleavage, flanking vector-encoded sequences have often been involved in either inhibition or enhancement of the ribozyme activity (7, 8, 14, 15). Here we describe a simple method to prepare RNA molecules containing only one nucleotide (a 5′ G required for efficient *in vitro* transcription) in addition to the desired sequence.

Synthetic DNA templates of up to 170 base-pairs were PCR-amplified and efficiently transcribed *in vitro* by T7 RNA polymerase. Sequencing of the transcription products showed that they corresponded to the expected transcripts. Moreover, by cloning the PCR-amplified templates and sequencing a large number of clones, we verified that the sequences corresponded to the designed oligonucleotides. Thus, this procedure provides a reliable, easy and rapid way to obtain relatively long templates for *in vitro* transcription, avoiding time-consuming steps, such as ligation and cloning, as well as addition of undesired vector flanking sequences in the final transcription products.

The second technical improvement concerns the synthesis of active RNA precursors. Ribozyme cleavage during transcription has often been reported for both virusoid and HDV self-cleaving fragments; in most cases, the residual full-length ribozymes, once purified, were unable to self-cleave, thus hindering the analysis of the corresponding cleavage reactions (7, 8,12,16). Transcription at 4°C provides a simple method to prepare active ribozymes that otherwise would be unavailable. First, the proportion of uncleaved ribozyme produced is higher when transcription is performed at 4°C compared to 37°C. Second, the fraction of Rz89 precursor which is not cleaved during transcription at 37°C remains uncleaved to 90% once purified, while 95–99% of Rz89 precursor transcribed at 4°C is further cleavable. The inability of Rz89 fraction to self-cleave may be due to 3′ modifications, since the RNA sequence upstream the 3′ end are correct. Therefore, transcription at low temperature seems to produce a lower level of enzymatic modification such as reported for RNA transcribed from both cloned and synthetic templates (20–23).

The structure of the HDV genomic ribozyme

The results presented in this paper further extend the delineation of the HDV minimal ribozyme structure. Rz71, carrying a deletion in the stable domain B stem-loop, is able to self-cleave, the half-time of the reaction at 37°C and 10 mM $MgCl_2$ being 3 min . Nevertheless, it is less efficient than Rz89, which under the same conditions is cleaved to 50% in less than 15 sec. In addition, while Rz 89 still cleaves very efficiently under severe denaturing conditions (90°C or in 7.5 M urea or 10 M formamide), Rz71 is active only up to 60°C or 5 M urea (G.T., unpublished results). These observations suggest that, even when domain B may not be directly involved in the catalytic core of the HDV ribozyme, it plays an important role in delivering the molecule to the active conformation and/or in stabilizing the active structure.

It is noteworthy that not only Rz89 and Rz71 are active under the above mentioned denaturing conditions, but also they are enhanced by them (Fig.4; F.L. and G.T., unpublished results). This indicates that the self-cleavage reaction admits, or even requires, a relative flexibility of the RNA molecule . The RNAFOLD analysis of Rz85 (−1/+84) and Rz133 (−35/+98) showed that the region corresponding to nt −1 to +40 (domain A, Fig.1-B), and particularly the sequence corresponding to stem-loop III in the pseudoknot-like structure (Fig. 1-A), is far less stable than domain B, being able to adopt slightly different structures in equilibrium with each other (data not shown). The conformational flexibility of stem-loop III makes it a good candidate for being directly involved in the catalytic core of the ribozyme.

SD106, an RNA fragment corresponding to positions −3 to +84 plus18 nt of 3′ vector encoded sequences, was reported to cleave less efficiently than Rz89 (−5/+84 plus a 5′G) under non-denaturing conditions ($t_{1/2}$ about 3.5 min at 37°C, ref. 15; compare to Rz89, $t_{1/2}$ <15 sec, Fig.3). Since only one nucleotide 5′ to the break site seems to be sufficient for SD106 self-cleavage (15), the kinetic differences are more probably due to the 3′ non-HDV sequences than to variations 5′ to the break site. The fact that Rz89 still self-cleaves efficiently at 90°C or 7.5 M urea, suggests that its active conformation is rather stable and, therefore, it is unlikely that inhibitory vector-derived sequences act by disrupting double-stranded regions of the HDV −3/+84 fragment. Alternatively, non-HDV sequences might interfere by interacting with single-stranded regions involved in catalysis. In this sense, it is interesting to note that a 5′CGAG3′ sequence found in the 3′ extension of SD106 (15) can base-pair with 3′GCUC5′ present in the terminal loop of stem III (Fig.1-A).

Based on the presented data, our working model of HDV minimal ribozyme is that the main role of domain B (stem IV in the pseudoknot structure) is structural, contributing to arrange correctly the structure of the catalytic core contained in domain A (stems I and III, and 5′ side of stem II in the pseudoknot model), but not being directly involved in catalysis. Concerning domain A, stem I may be regarded as containing the substrate on the 5′ side and, on the 3′ side, a guide sequence similar to that described for group I intron splicing (25); finally the active-site chemistry may be mediated by stem-loop III. Further mutagenesis and deletion studies of Rz71 will help us to better dissect the HDV ribozyme conformational requirements.

ACKNOWLEDGMENTS

We are specially grateful to F. Baudin, B. Ehresmann and C. Ehresmann for the RNAFOLD analysis of HDV sequences. This work was supported in part by grants from ARC, LNCC, ANRS and MEN (Virologie Fondamentale). G.T. is recipient of a CIFFRE fellowship from MRT.

REFERENCES

1. Rizzetto, M., Canese, M.G., Arico, J., Crivelli, O., Bonino, F., Trepo, C.G. and Verme, G. (1977) *Gut*, **18**, 997–1003.
2. Wang, K.-S., Choo, Q.-L., Weiner, A.J., Ou, J.-H., Najarian, R.C., Thayer, R.M., Mullenbach, G.T., Denniston, K.J., Gerin, J.L. and Houghton, M. (1986) *Nature*, **323**, 508–514.
3. Kos, A., Dijkema, R., Arnberg, A.C., van der Meide, P.H. and Schellekens, H. (1986) *Nature*, **323**, 558–560.
4. Chen, P.-J., Kalpana, G., Goldberg, J., Mason, W., Werner, B., Gerin, J. and Taylor, J. (1986) *Proc. Natl. Acad. Sci.* USA, **83**, 8774–8778.
5. Taylor, J.M. (1991) *Curr. Top. Microbiol. Immunol.* **168**, 141–166.
6. Sharmeen, L., Kuo, M.Y.-P., Dinter-Gottlieb, G. and Taylor, J. (1988) *J. Virol.*, **62**, 2674–2679.
7. Kuo, M.Y.-P., Sharmeen, L., Dinter-Gottlieb, G. and Taylor, J. (1988) *J.Virol.*, **62**, 4439–4444.

8. Wu, H.-N., Lin, Y.-J., Lin, F.-P., Makino, S., Chang, M.-F. and Lai, M.M.C. (1989) *Proc. Natl. Acad. Sci.* USA, **86**, 1831–1835.
9. Sharmeen, L., Kuo, M.Y.-P. and Taylor, J. (1989) *J. Virol.*, **63**, 1428–1430.
10. Taylor, J., Sharmeen, L., Kuo, M. and Dinter-Gottlieb, G. (1989) In Cech, T. (ed.), Molecular Biology of RNA. A. Liss, New York, pp. 99–108.
11. Rosenstein, S.P. and Been, M.D. (1990) *Biochemistry*, **29**, 8011–8016.
12. Wu, H.-N and Lai, M.M.C. (1990) *Mol. Cell. Biol.*, **10**, 5575–5579.
13. Smith, J.B. and Dinter-Gottlieb, G. (1991) *Nucl. Acids Res.*, **19**, 1285–1289.
14. Belinsky, M.G. and Dinter-Gottlieb, G. (1991) *Nucl. Acids Res.*, **19**, 559–564.
15. Perrotta, A.T. and Been, M.D. (1990) *Nucl. Acids Res.*, **18**, 6821–6827.
16. Forster, A.C. and Symons, R.H. (1987) *Cell*, **49**, 211–220.
17. Hampel, A., Tritz, R., Hicks, M. and Cruz, P. (1990) *Nucl. Acids Res.*, **18**, 299–304.
18. Perrotta, A.T. and Been, M.D. (1991) *Nature*, **350**, 434–436.
19. Sambrook, J., Fritsch, E.F. and Maniatis, T. (1989) Molecular Cloning: A Laboratory Manual. 2nd Ed. Cold Spring Harbor Laboratory Press, Cold Spring Harbor.
20. Milligan, J.F. and Uhlenbeck, O.C. (1989) *Methods in Enzymology*, **180**, 51–62.
21. Schenborn, E.T. and Mierendorf, R.C. Jr. (1985) *Nucl. Acids Res.*, **13**, 6223–6236.
22. Konarska, M.M. and Sharp, P.A. (1989) *Cell*, **57**, 423–431.
23. Milligan, J.F., Groebe, D.R., Witherell, G.W. and Uhlenbeck, O.C. (1987) *Nucl. Acids Res.*, **15**, 8783–8798.
24. Zuker, M. (1989) *Science*, **244**, 48–52.
25. Davies, R.W., Waring, R.B., Ray, J.A., Brown, T.A. and Scazzocchio, C. (1982) *Nature*, **300**, 719–724.